

TRANSFORMATION OF SYNTHETIC BIRNESSITE TO CRYPTOMELANE: AN ELECTRON MICROSCOPIC STUDY

CY-CHAIN CHEN, D. C. GOLDEN, AND J. B. DIXON

Department of Soil & Crop Sciences, Texas A&M University
College Station, Texas 77843

Abstract—Na-saturated birnessite was synthesized by oxidizing an alkaline MnCl_2 solution with gaseous O_2 . Transmission electron microscopy (TEM) showed no morphological change upon K-saturation of the birnessite, but selected-area diffraction (SAD) revealed structural disorder. Stepwise heating of the K-birnessite to 800°C yielded cryptomelane, as indicated by X-ray powder diffraction (XRD). Various degrees of transformation to the final cryptomelane product were observed by TEM and SAD, but not by XRD. Unaltered birnessite formed chiefly as thin, platy crystals of apparent hexagonal outline. The cryptomelane crystals that formed by heating the K-saturated birnessite were acicular. Birnessite crystals, partially transformed to cryptomelane and displaying non-integral diffraction spots, formed plates having linear striations and rods twinned at 60° to each other. These intermediate products commonly retained some of the original hexagonal appearance of the parent birnessite. Structural disorder was detected in the partially transformed crystals by SAD. TEM revealed 6.8- and 4.8-Å spacings of the (110) and (200) planes of cryptomelane, respectively. The basal planes of birnessite layers (001) appeared to correspond topotactically to the (110) plane of cryptomelane during these transformations.

Key Words—Birnessite, Cryptomelane, Selected area diffraction, Structural disorder, Synthesis, Thermal treatment, Transmission electron diffraction.

INTRODUCTION

Birnessite ($\text{Na}_4\text{Mn}_{14}\text{O}_{27}\cdot 9\text{H}_2\text{O}$) is common in natural systems (Giovanoli, 1980) and is the most common manganese oxide in soils (Dixon *et al.*, 1986). It has a layered structure composed of alternately stacked sheets of MnO_6 octahedra linked through oxygen ions and water molecules which occupy the interlayers. Synthetic birnessite transforms into other manganese oxides at elevated temperatures. The products of such transformations appear to be determined by the nature of saturating cation. K-saturated birnessite, for example, transforms gradually to cryptomelane upon heating (Golden *et al.*, 1986b). Cryptomelane ($\text{K}_2\text{Mn}_8\text{O}_{16}$) is a tunnel-type structure in which double chains of octahedra are connected through oxygen ions at edges to form the tunnels which contain the K^+ (Post *et al.*, 1982). Faulring *et al.* (1960) reported the topotactic transformation of cryptomelane to bixbyite and the subsequent transformations to hausmannite and spinel upon heating. Understanding the crystallographic relations between birnessite and cryptomelane will illuminate further this thermal transformation series.

The following investigation was carried out to examine in detail the intermediate products that form during the transformation of birnessite to cryptomelane by K-saturation and heating and to determine the morphological and crystallographic relations between reactants and products.

MATERIALS AND METHODS

Oxygen gas was passed through 100 ml of 0.5 M MnCl_2 solution in a 500-ml plastic beaker at a rate of 1.7 liter/min by means of a glass frit. After 5 min, 125 ml of 6 N NaOH was added while stirring the solution slowly. Oxygenation and stirring were continued for 5 hr. Soluble ions were removed from the black precipitate by repeated centrifugations and washings with water, followed by dialysis against water. Subsequent freeze drying yielded birnessite as a black powder.

The original sample had a cation-exchange capacity (CEC) of 256 meq/100 g. The original cation balancing the negative charges was Na^+ . The Na^+ was replaced with K^+ by washings with 1 N KCl solution followed by the salt-removal procedures. The K-saturated sample was mounted on a Vycor glass slide and heated in a step-wise fashion at 200°, 400°, 600°, and 800°C for 2 hr at each step. X-ray powder diffraction (XRD) analyses were made of the original Na- and K-saturated birnessites and the heated samples after each heating step using $\text{CuK}\alpha$ radiation and a Philips Norelco XRD unit equipped with a graphite monochromator.

The Na- and K-saturated birnessites and the heated (800°C) samples were dispersed and diluted before mounting on a Cu grid covered with a carbon-coated Formvar film. For high-resolution transmission electron microscopy (HRTEM), a holey carbon grid fabricated using a Microgrid kit (Okem Shoji Kabushiki Kaishya, Tokyo, Japan) was used. A Zeiss 10C TEM

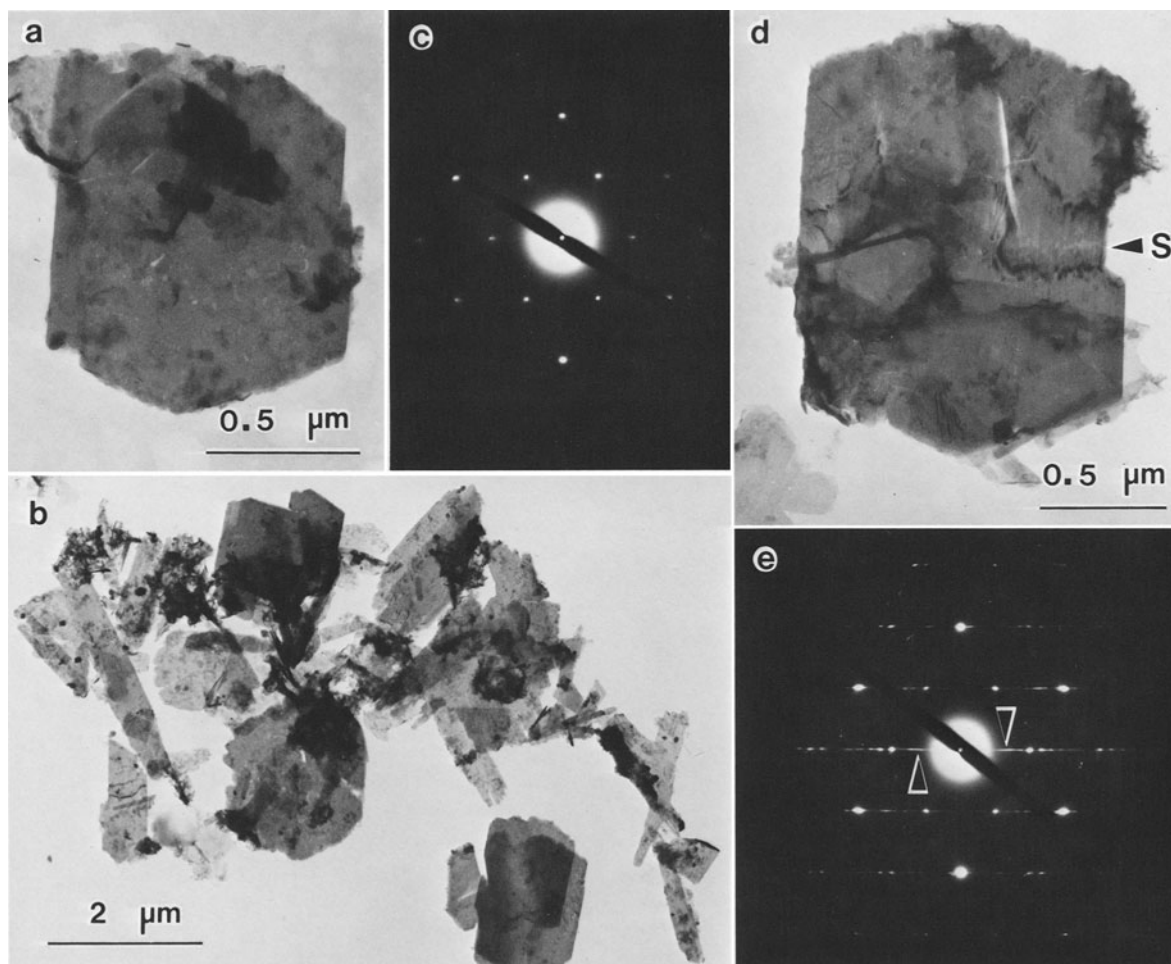


Figure 1. Transmission electron micrographs of: (a) synthetic Na-birnessite single crystal; (b) synthetic Na-birnessite aggregate; (c) selected-area diffraction (SAD) pattern of crystal shown in (a); (d) single crystal of K-saturated-birnessite; (e) SAD pattern of crystal shown in (d).

operated at 60 kV was used for morphological and selected-area diffraction (SAD) observations. HRTEM micrographs were obtained using the same instrument operated at 100 kV.

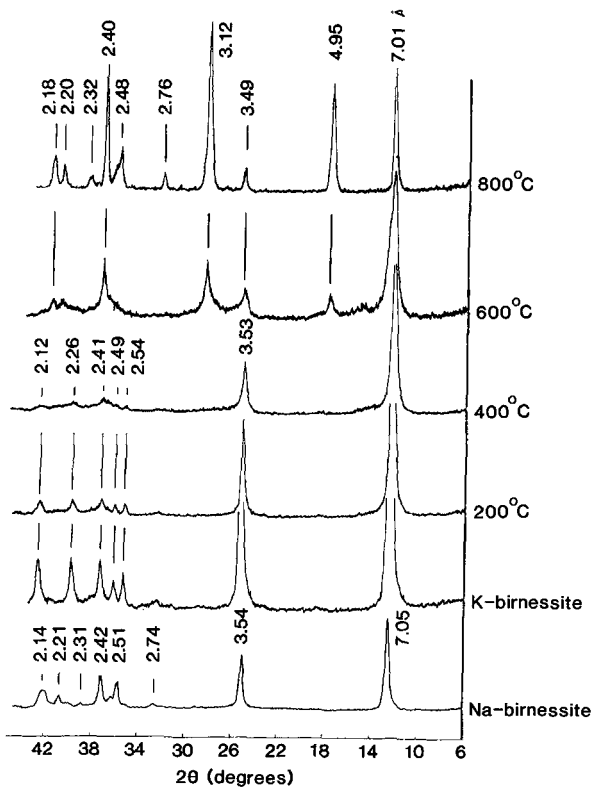
RESULTS AND DISCUSSION

Na-saturated birnessite typically crystallized as thin plates of pseudo-hexagonal outline with two parallel edges smoother than the other four (Figure 1a). Some laths also formed (Figure 1b). SAD of a single crystal (Figure 1c) yielded a spot pattern having an apparent 6-fold rotational axis of symmetry. First-order diffraction spots in the pattern indicate a d -value of 1.45 Å.

No morphological changes were noted after K^+ saturation, however, some particles developed striations (S, Figure 1d), but not enough to be attributed conclusively to the K-saturation. The striations on the crystal shown in Figure 1d appear to be parallel to the smoother sides of the crystal. The SAD pattern (Figure 1e) suggests structural disorder, presumably induced by the K-saturation. The SAD pattern of birnessite remained after K-saturation, but was more diffuse, as shown in Figure 1e. In addition to the original birnessite SAD pattern, spots having large d -values (~ 2.5 Å, arrowheads, Figure 1e) indicate the presence of superlattices intersecting the birnessite octahedral sheets.

Figure 3. Transmission electron micrographs of: (a) cryptomelane single crystal; (b) selected-area diffraction (SAD) pattern of crystal shown in (a); (c) crystal incompletely transformed from birnessite to cryptomelane (note linear striations); (d) SAD pattern of crystal shown in (c); (e) crystals incompletely transformed from birnessite to cryptomelane showing striations in three directions; (f) similar crystals as in (e) occurring as twinned rods; (g) aggregate of cryptomelane crystals.

→

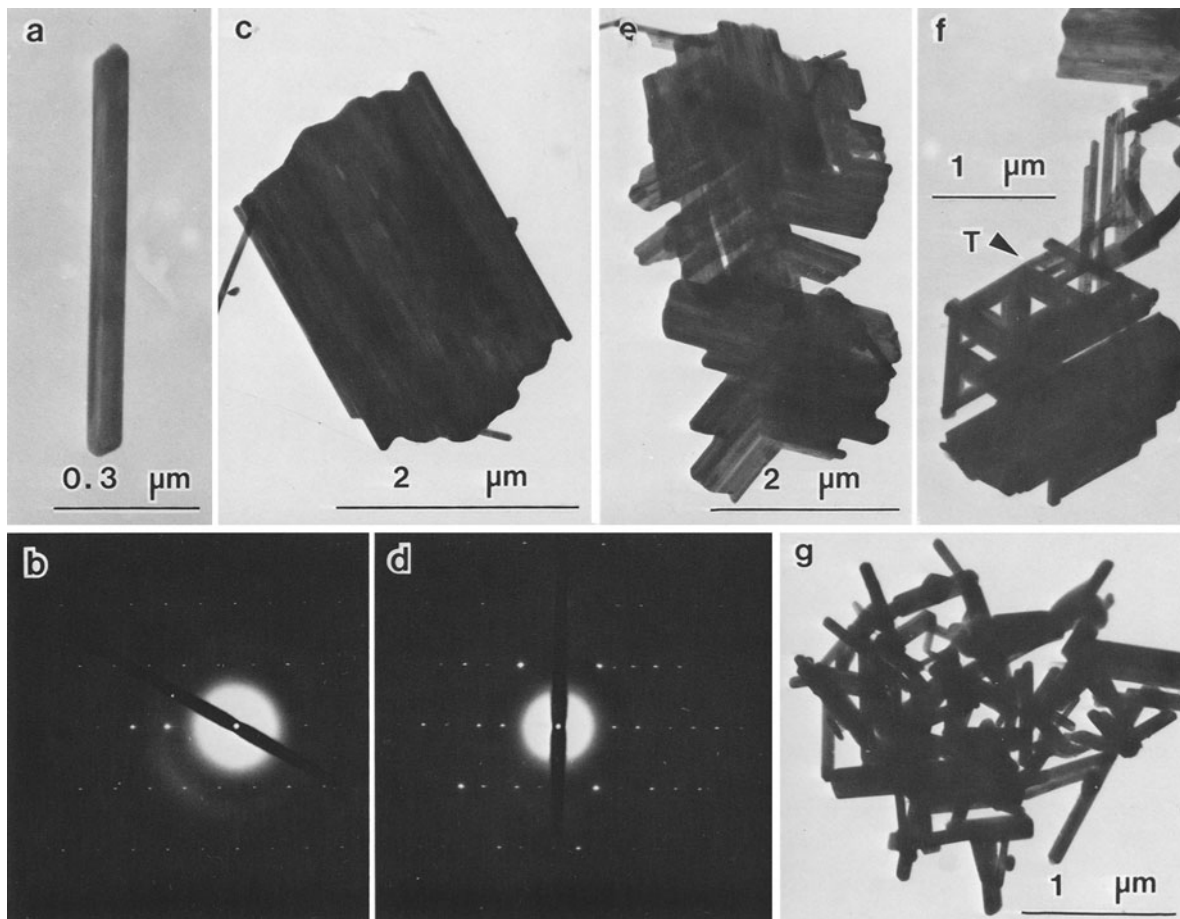


These observations suggest that some one-directional structural rearrangement has taken place.

The structural disorder suggested by the SAD pattern is reflected in the XRD pattern as well (Figure 2). The XRD peaks of Na-birnessite agree well with the literature values for peak positions and relative intensities (JCPDS 23-1045). After K-saturation, the major peaks were unchanged; however, the positions and relative intensities of minor peaks in the 2–3-Å region changed, suggesting that K-saturation caused structural changes even prior to the heat treatment. Thus, the 3.54-Å (002) birnessite XRD peak does not appear to represent the same structural feature as revealed by the 3.54-Å electron diffraction spacings shown in Figure 1e. Preferred orientation apparently caused the basal planes of the birnessite crystals to lie perpendicular to the electron beam; thus, basal spacings were not detected by SAD. The 3.5-Å electron diffraction spacing is therefore likely due to new atomic planes oriented roughly perpendicular to the birnessite layers.

←

Figure 2. $\text{CuK}\alpha$ X-ray powder diffraction patterns of synthetic Na-birnessite and the products of K-saturation and heat treatments. Temperatures = temperatures of heat treatment. d-values on patterns are in Å.



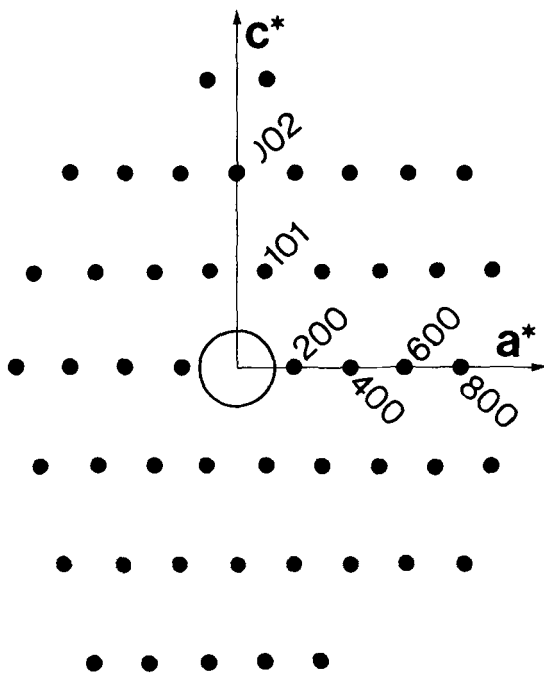


Figure 4. Indexed selected-area diffraction pattern traced from Figure 3b.

Treatments at 200° and 400°C yielded intermediate products. XRD peaks in the 2–3-Å region gradually weakened until they were almost absent in the XRD pattern of the sample heated to 400°C (Figure 2). At 600°C, the major peaks of cryptomelane were all present. At 800°C, the minor peaks of cryptomelane were also present, and the 4.95-, 3.12-, and 2.40-Å major peaks were more intense with respect to the 7.01-Å peak. All of these peaks appear to belong to cryptomelane, except the 2.76-Å peak. The 2.76-Å peak and part of the 2.48-Å peak appear to be the 85 (103) and 100 (211) intensity peaks of hausmannite (JCPDS 24-734), respectively. The formation of hausmannite is discussed below.

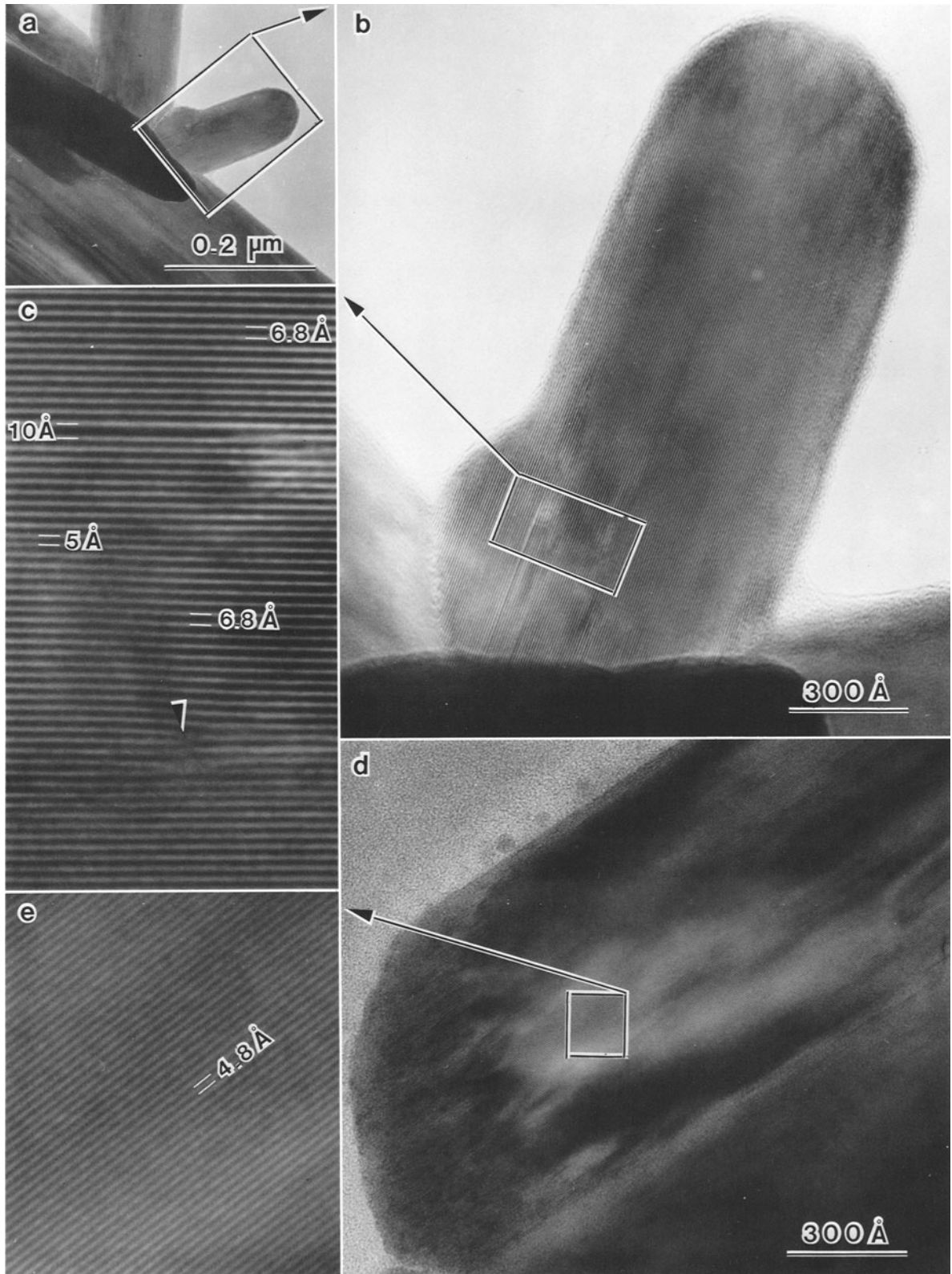
Electron micrographs show that the degree of transformation of birnessite to cryptomelane varied among individual particles. Consider, for example, the SAD pattern of the acicular crystal of cryptomelane in Figure 3a is shown in Figure 3b. Assuming tetragonal symmetry for cryptomelane, the SAD pattern shows the a^*c^* plane (Figure 4). The SAD patterns of non-acicular particles in Figure 3c suggest incomplete trans-

formations, but these intermediate states were not detected by XRD. In Figure 3c parallel striations can be seen on particles showing vestiges of a hexagonal outline. The SAD pattern of the particle shown in Figure 3d contains abundant non-integral diffraction spots that suggest disorder or the presence of a superlattice which is manifested as striations. Three directions of striations intersecting at 60° appear to be present on a plate shown in Figure 3e. The plates also appear to transform into twinned rods (T, Figure 3f). The rods are aligned with one of the three striation directions of the birnessite plate described above. Such a trilling pattern was reported for todorokite by Turner and Buseck (1981). This particle has apparently retained the hexagonal outline of the parent birnessite crystal (T, Figure 3f). Some rods occur as randomly oriented aggregates (Figure 3g). The abundance of these two different morphologies (cf. Figures 3e and 3g) is about the same.

Obtaining the lattice fringes of these crystals was difficult due to their thickness. Only a few rods, such as those shown in Figure 5a, were suitable for imaging. The measured d -value of 6.8 Å corresponds to the (110) planes of cryptomelane (Figure 5b); hence, the crystallographic axes of the parent birnessite and the daughter cryptomelane are apparently related. As shown in Figure 6, cryptomelane may be considered to contain two sets of parallel octahedral sheets intersecting each other at 90°. The vertical set results in the observed lattice image shown in Figure 5b, whereas the horizontal set is parallel to the plane of view and equivalent to the octahedral sheets of birnessite. The transformation may take place by “pillaring,” as suggested by Arrhenius and Tsai (1981) between birnessite sheets. Most of the birnessite layers appear to have remained intact during the transformation, thereby preserving part of their hexagonal outline. Golden *et al.* (1986a) observed a similar preservation of crystal morphology in the transformation of birnessite to todorokite under hydrothermal conditions. The pillars, consisting of MnO_6 octahedra, eventually coalesced to form the vertical set of octahedral sheets of the cryptomelane structure. The large size of the K^+ ion may have helped prevent the birnessite layers from collapsing during the heating process.

Only limited lattice irregularity can be seen in Figure 5c, as evidenced by the few 5- and 10-Å fringes among the predominantly 6.8-Å lattice fringes. A termination of a lattice fringe is visible at the arrowhead in this figure. The d -value of 4.8 Å probably represents the

Figure 5. (a) Transmission electron micrograph of part of twinned cryptomelane crystal. (b) High-resolution transmission electron microscopic image of crystal shown in (a). (c) Enlargement of area shown in (b). (d) High-resolution transmission electron microscopic image of cryptomelane crystal. (e) Enlargement of area shown in (d).



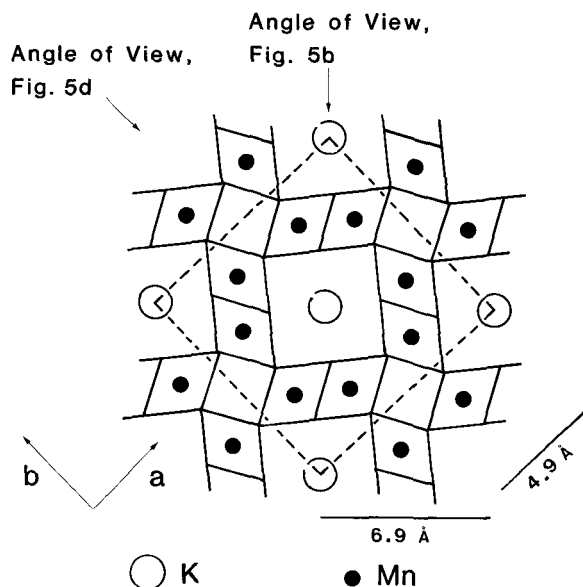


Figure 6. Crystal structure of cryptomelane (from Post *et al.*, 1982).

(200) planes of cryptomelane (Figures 5d and 5e). The geometry required to reveal the (110) and (200) planes is shown in Figure 6. The d -values are slightly less than literature XRD values of 6.9 and 4.9 Å for cryptomelane (JCPDS 20-908).

An additional interpretation of the 4.8-Å spacings is possible. If the large K ion is absent during such a transformation, a structure similar to that of hausmannite ($d(110) = 4.9$ Å) may form (Golden *et al.*, 1986b). The 256-meq/100 g of exchangeable K^+ in

birnessite translates to a K:Mn ratio of 1:3.2, more than enough K^+ for the ideal 1:4 K:Mn ratio of cryptomelane. At 800°C, however, K may have been expelled and volatilized locally from the cryptomelane and allowed hausmannite to have formed in this product. Lattice fringes shown in Figure 7 support this interpretation. Both the 6.8- and 4.8-Å spacings (H and L, respectively, Figures 7b and 7c) are visible in the same plane. The 4.8-Å spacings are located near the edge of the crystal where presumably K would have been expelled first. A region of disordered lattice fringes exists between the regular 6.8- and 4.8-Å regions (R, Figures 7b and 7c).

SUMMARY AND CONCLUSIONS

Birnessite transformed into cryptomelane upon K-saturation and heating. Crystallographic rearrangement began with the K-saturation and proceeded gradually with heating to 800°C. The relative crystallographic orientation during the transformation was birnessite (001) = cryptomelane (110). The transformation was incomplete in some crystals even after the 800°C heat treatment, as noted by TEM and SAD. XRD analysis of bulk samples gave no evidence of such incomplete transformation.

The data obtained in this study suggest that the cryptomelane formed by the "pillaring" of MnO_6 octahedra between birnessite octahedral sheets. This process yielded the "2 octahedra \times 2 octahedra" tunnel structure of cryptomelane. The K ions seem to have acted as spacers between the birnessite octahedral sheets and, therefore, were the most important factors in controlling the size of the tunnels.

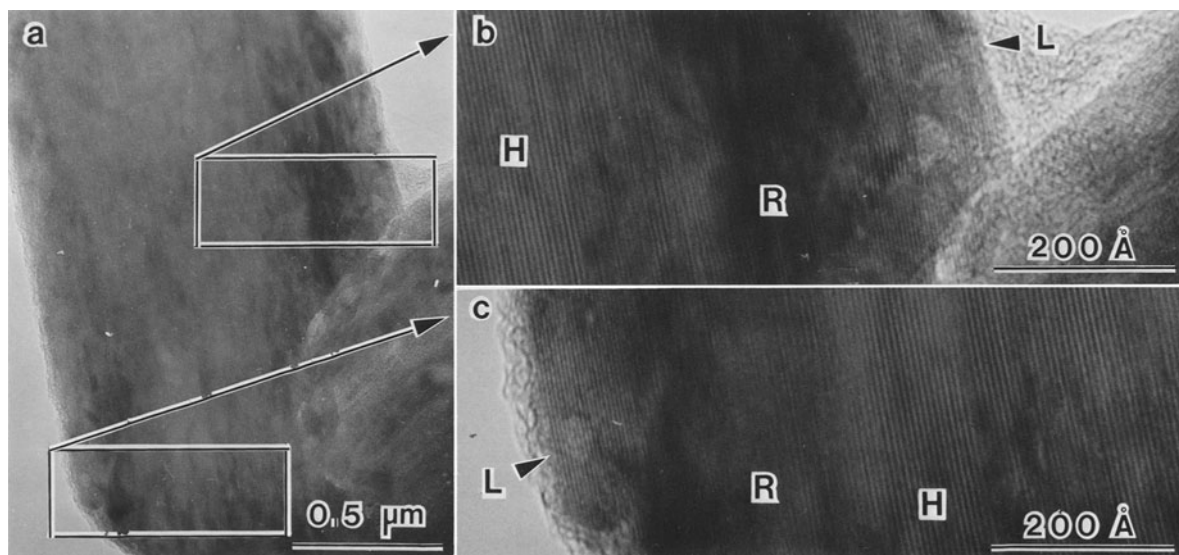


Figure 7. (a) High-resolution electron microscopic image of cryptomelane. (b) and (c) enlargements of areas shown in (a). H = 6.8-Å region; L = 4.8-Å region; R = disordered region.

ACKNOWLEDGMENTS

The authors express their appreciation to P. R. Buseck and D. W. Ming for constructive review comments and to the Electron Microscopy Center at Texas A&M University for use of its facilities. This manuscript was approved as Texas Agricultural Experiment Station technical article No. 21126.

REFERENCES

- Arrhenius, G. O. and Tsai, A. G. (1981) Structural, phase transformation and prebiotic catalysis in marine manganese minerals: Scripps Inst. Ocean., La Jolla, California, *SIO Ref. Series* **81-28**, 1-19.
- Dixon, J. B., Golden, D. C., Uzochukwu, G. A., and Chen, C. C. (1986) Soil manganese oxides: in *Soil Colloids, Structures, and Associations in Soil Aggregates*, M. H. B. Hayes and A. Herbillon, eds. NATO Workshop, Ghent, Belgium, (in press).
- Faulring, G. M., Zwicker, W. K., and Forgeng, W. D. (1960) Thermal transformations and properties of cryptomelane: *Amer. Mineral.* **45**, 946-959.
- Giovanoli, R. (1980) On natural and synthetic manganese nodules: in *Geology and Geochemistry of Manganese, Vol. 1*, I. M. Varentsov and G. Grasselly, eds., Hungarian Acad. Sci., Budapest, 160-202.
- Golden, D. C., Chen, C. C., and Dixon, J. B. (1986a) Synthesis of todorokite: *Science* **231**, 717-719.
- Golden, D. C., Dixon, J. B., and Chen, C. C. (1986b) Ion-exchange, thermal transformation, and oxidizing properties of birnessite: *Clays & Clay Minerals* **34**, 511-520.
- Post, J. E., Von Dreele, R. B., and Buseck, P. R. (1982) Symmetry and cation displacements in hollandite: structure refinements of hollandite, cryptomelane, and priderite: *Acta Crystallogr.* **B38**, 1056-1065.
- Turner, S. and Buseck, P. R. (1981) Todorokite: a new family of naturally occurring manganese oxides: *Science* **212**, 1024-1027.
- (Received 2 December 1985; accepted 22 March 1986; Ms. 1545)